

The Principle and Simulation of Magnetic Coupling for Rectangular Coil in Mobile Payment System

Yejun He, Xiaorong Tang, Jie Yang and Jiefeng Ao

College of Information Engineering
Shenzhen University
Shenzhen, China
Email:heyeyun@ieee.org

Abstract—In this paper, we propose a new magnetic field coupling scheme which is applied in mobile payment system. The coil coupling model of mobile payment system with the 2kHz is established. Based on the principle of magnetic flux variation, we calculate and analyze the magnetic flux density and the coupling voltage in different distances. We mainly simulate the relationship between the coupling voltage and the distance from the transmit coil to the coupling coil and that between the coupling voltage and some different excitation signals.

Keywords—mobile payment; radio frequency identification; magnetic coupling

I. INTRODUCTION

Mobile payment is usually known as the electronic wallet. It is a kind of accounting transaction way for mobile users to use mobile phones to pay for the goods or services. Mobile payment was characterized as event-based applications by some scholars[1]. According to the latest study from Juniper Research, the mobile payment market will reach \$600 billion in 2013 [2]. Therefore, the mobile payment occupied an important position in the mobile business affairs and wireless applications, which is a research hotspot in recent years [3-9]. Mobile payment is firstly used in Japan, Korea, Singapore, Austria as well as Norway.

The field of mobile payment is used lately in China. The industrial chain direction of mobile payments is mainly led by China Mobile, and other related companies provide dedicated SIM card. At present, mobile users only need to launch their mobile wallets in the Hall of China Mobile, in other words, a dedicated RFID-enabled SIM card needs to be installed [10]. Then, we can use the mobile phone to consume in some places with China Mobile dedicated POS machines. The coupling coil discussed in this paper is installed in the dedicated SIM card with the RFID function while the transmit coil is placed on the China Mobile dedicated POS machine. A typical RFID application involves the use of RFID tags, RFID readers and a terminal system. RFID technology is widely used in industrial automation, business automation, traffic control and management, security and many other fields [11-13], and is also the key technology of Internet of things. Most of the radio frequency identification systems are based on the principle of

inductive coupling. Therefore, it is necessary to understand the energy and data transfer process between the reader (equipped with a transmit coil) and the transponder (equipped with a coupling coil) and to study the physical nature in the phenomena. Electromagnetic theory from the perspective of RFID is studied in this paper.

The rest of this paper is organized as follows. In Section II, we briefly illustrate the magnetic coupling model in the mobile payment system. In Section III, we calculate and analyse the magnetic induction around the transmit coil of the mobile payment system. In Section IV, we study the coupling voltage based on the principle of magnetic coupling. Conclusions are in Section V. Note: In this paper, the distance from transmit coil to coupling coil (or called “height”) is in the z-axis direction.

II. THE MAGNETIC COUPLING MODEL IN MOBILE PAYMENT SYSTEM

Nationz Technologies Co., Ltd. in China developed the first generation readers, which use 2.4GHz to communicate and 2.4GHz to control a distance. However this method has some shortcomings for some mobile phones when it controls the distance. The lower the frequency is, the longer the wavelength is, and the signal can penetrate most of the materials. In view of this, we propose a new generation of distance control method using the principle of magnetic coupling together with this company. This new method is based on the coupling voltage which controls the distance between the reader and the transponder in low frequency (2kHz). The basic principle is similar to RFID technology in 125kHz and 13.56MHz using near field communication. As shown in Fig.1, electromagnetic coupling between the reader coil (called transmit coil in this paper) and the transponder exists. When the transponder goes into the alternative magnetic field generated by the reader, the transponder coil will produce an induction voltage. When the distance is close enough, the induction voltage will reach a certain threshold. Then the information will be certified and interacted, and the car payment is finished. The shape of the transmit coil and the coupling coil are all rectangular. The signal source in the transmit coil is not the current but the voltage. We conduct a theoretical analysis, simulation and field testing for the method. The method applied to the test system shows good security and high robustness.

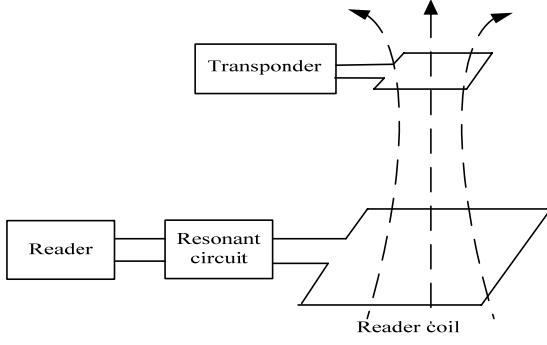


Fig. 1 A reader system

The instantaneous induction voltage v_2 in the coupling coil of the transponder is proportional to the variation rate of the total flux Ψ across the conductor. The induction voltage can be expressed as:

$$v_2 = -\frac{d\Psi}{dt} = -N_2 \frac{d\phi}{dt} \quad (1)$$

where N_2 denotes the number of turns in the coupling coil of transponder, and ϕ is the flux of each turn of the coil.

The transponder card is used to detect the amplitude of v_2 and as a threshold of the distance control.

III. MAGNETIC FLUX DENSITY OF THE SPACE AROUND THE RECTANGULAR TRANSMIT COIL

Regarding the rectangular current-carrying coil as four current-carrying straight wire sub-calculated, we will get the space magnetic field distribution of rectangular current-carrying coil after the magnetic field intensity of each segment is superposed. The center of the rectangular current-carrying coil is the coordinates of the origin. Setting $AB = 2l_1$, $BC = 2l_2$, and the coordinates of the field point is P (x, y, z). Firstly we calculate the magnetic flux density generated by BC at P. Crossing the P-point to do a straight line perpendicular to BC, we get the crossover point Q in BC as shown in Fig.2.

By calculation, the three components of magnetic flux density in the space in the current-carrying rectangular coil are as follows:

$$B_x = \frac{\mu_0 I z}{4\pi [(l_1 - x)^2 + z^2]} \left[\frac{l_2 + y}{\sqrt{(l_1 - x)^2 + (l_2 + y)^2 + z^2}} + \frac{l_2 - y}{\sqrt{(l_1 - x)^2 + (l_2 - y)^2 + z^2}} \right] - \frac{\mu_0 I z}{4\pi [(l_1 + x)^2 + z^2]} \left[\frac{l_2 - y}{\sqrt{(l_1 + x)^2 + (l_2 - y)^2 + z^2}} + \frac{l_2 + y}{\sqrt{(l_1 + x)^2 + (l_2 + y)^2 + z^2}} \right] \quad (2)$$

$$B_y = \frac{\mu_0 I z}{4\pi [(l_2 - y)^2 + z^2]} \left[\frac{l_1 - x}{\sqrt{(l_1 - x)^2 + (l_2 - y)^2 + z^2}} + \frac{l_1 + x}{\sqrt{(l_1 + x)^2 + (l_2 - y)^2 + z^2}} \right] - \frac{\mu_0 I z}{4\pi [(l_2 + y)^2 + z^2]} \left[\frac{l_1 + x}{\sqrt{(l_1 + x)^2 + (l_2 + y)^2 + z^2}} + \frac{l_1 - x}{\sqrt{(l_1 - x)^2 + (l_2 + y)^2 + z^2}} \right] \quad (3)$$

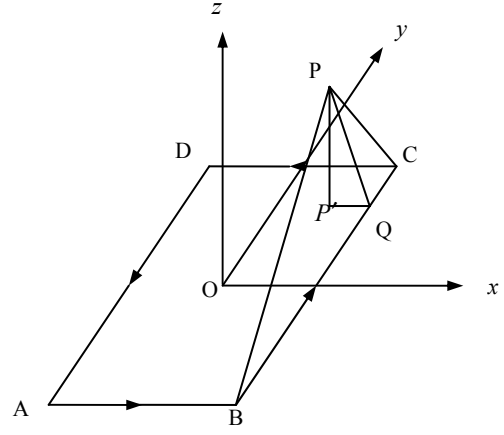


Fig. 2 Calculation of magnetic flux density of the rectangular coil

$$B_z = \frac{\mu_0 I (l_2 + y)}{4\pi [(l_2 + y)^2 + z^2]} \left[\frac{l_1 + x}{\sqrt{(l_1 + x)^2 + (l_2 + y)^2 + z^2}} + \frac{l_1 - x}{\sqrt{(l_1 - x)^2 + (l_2 + y)^2 + z^2}} \right] + \frac{\mu_0 I (l_2 - y)}{4\pi [(l_2 - y)^2 + z^2]} \left[\frac{l_1 - x}{\sqrt{(l_1 - x)^2 + (l_2 - y)^2 + z^2}} + \frac{l_1 + x}{\sqrt{(l_1 + x)^2 + (l_2 - y)^2 + z^2}} \right] + \frac{\mu_0 I (l_1 - x)}{4\pi [(l_1 - x)^2 + z^2]} \left[\frac{l_2 + y}{\sqrt{(l_1 - x)^2 + (l_2 + y)^2 + z^2}} + \frac{l_2 - y}{\sqrt{(l_1 - x)^2 + (l_2 - y)^2 + z^2}} \right] + \frac{\mu_0 I (l_1 + x)}{4\pi [(l_1 + x)^2 + z^2]} \left[\frac{l_2 - y}{\sqrt{(l_1 + x)^2 + (l_2 - y)^2 + z^2}} + \frac{l_2 + y}{\sqrt{(l_1 + x)^2 + (l_2 + y)^2 + z^2}} \right] \quad (4)$$

Substituting (2) to (4) into the following formula:

$$B = \sqrt{B_x^2 + B_y^2 + B_z^2} \quad (5)$$

we can obtain the magnetic flux density at point P. When $x = 0$ and $y = 0$, we can obtain the magnetic flux density produced by a current-rectangular coil on the distance along the z axis.

$$B = \frac{N_1 \mu_0 I l_1 l_2}{\pi} \left(\frac{1}{(l_2^2 + z^2) \sqrt{l_1^2 + l_2^2 + z^2}} + \frac{1}{(l_1^2 + z^2) \sqrt{l_1^2 + l_2^2 + z^2}} \right) \quad (6)$$

where I is the current of coil, N_1 is the number of turns of transmit coil, μ_0 is the permeability of free space and equals $4\pi \times 10^{-7}$, l_1 and l_2 are the half of length and width of rectangular coil, respectively.

If $z^2 \gg l_1^2 + l_2^2$, the magnetic flux density is

$$B = \frac{2N_1 \mu_0 I l_1 l_2}{\pi} z^{-3} \quad (7)$$

Equation (7) shows that when the height of the coupling coil is much larger than half of the diagonal of the rectangular coil, the magnetic flux density is attenuated by z^{-3} as the height of the coupling coil increases.

When the transmit coil inputs a DC voltage, it will produce a stable magnetic field and the coil flux will not change. Consequently, there will be no induction EMF and induction current. Therefore, when it is in a steady state, there is no electromagnetic energy conversion and the coil is purely resistive. When the coil is exerted by an AC voltage, alternating current is generated which results in alternating magnetic force. By the principle of electromagnetic induction the transmit coil will detect the alternating electromotive force. The transmit coil is regarded as the energy storage components.

The effective value of the AC current in transmit coil is

$$I = \frac{U}{\sqrt{R^2 + (\omega L)^2}} \quad (8)$$

where $\omega = 2\pi f$.

The resistance of the rectangular transmit coil is

$$R = N_1 \rho \frac{l}{S} = N_1 \rho \frac{4(l_1 + l_2)}{\pi a_0^2} \quad (9)$$

where ρ is the resistivity of wire. The coil is generally made of copper wire whose resistivity is $1.7 \times 10^{-8} \Omega \cdot m$. l is the coil's perimeter. S is the area of the wire's cross section. a_0 is the radius of the wire's cross section. The inductance of rectangular coil is calculated as follows[14]

$$L = \frac{0.0276(CN_1)^2}{1.908C + 9b + 10h} \quad \mu H \quad (10)$$

where $C = x + y + 2h$, x is the width of coil, y is the length of coil, h is the height of the coil's cross section. b is the width of the coil's cross section. All dimensions are in cm.

IV. COUPLING VOLTAGE BASED ON THE PRINCIPLE OF MAGNETIC COUPLING

According to the principle of magnetic flux, when the input current in the transmit coil is a sine wave, the peak induction voltage in the coupling coil is calculated as follows [14].

$$V_0 = 2\pi f N_2 Q S B \cos \alpha \quad (11)$$

where f is frequency of arrival signal, N_2 is number of turns of the coupling coil, Q is quality factor of the resonant circuit, S is area of the coupling coil, B is the strength of crossing the coupling coil(or the arrival signal), and α is the angle between the transmit coil and coupling coil.

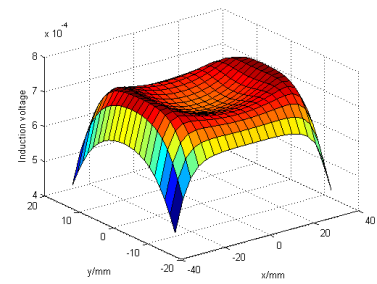
When the input current of transmit coil is a triangle wave, the peak induction voltage of the coupling coil is calculated as follows.

$$V_0' = 4f N_2 Q S B \cos \alpha \quad (12)$$

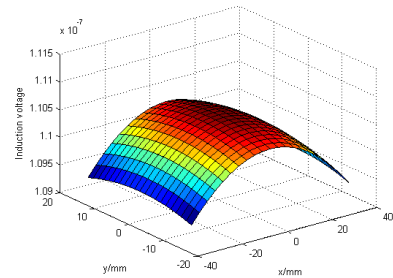
The system studied in this paper is not involved in a resonant network of the coupling coil, so the quality factor of the resonant circuit is 1. When the transmit coil is parallel to the coupling coil, the angle between transmit coil and coupling coil is 0. Substituting (5) into (12), we can obtain the induction voltage of coupling coil anywhere as shown in Fig.3. The simulation parameters are set as follows: the length of rectangular transmit coil is 70mm, the width of rectangular transmit coil is 30mm, the height of the coil's cross section is 1.6mm, the width of the coil's cross section is 8mm and the number of turns is 250, the voltage amplitude in transmit coil is 1V, the signal waveform is triangular wave with a frequency of 2kHz, the length of rectangular coupling coil is 24mm, the width is 14mm, and the number of turns is 4.

Fig.3 shows the distribution of induction voltage of the coupling coil in two different height anywhere. Fig.4 shows the distribution curve of the induction voltage's amplitude at the segments which are parallel to transmit coil. Fig.5 shows the decay curve of the induction voltage's amplitude at the segments which are perpendicular to transmit coil.

Fig.3 (a) illustrates that when the coupling coil is close to the transmit coil at a distance of 10mm, there is a raised rectangle in the z-plane, and the size of the rectangle is exactly equal to the size of a rectangular transmit coil. It means that there is a maximum induction voltage near the transmit coil. In other words, the closer to the transmit coil the coupling coil is, the greater its coupling voltage is. In Fig.3 (b), when the coupling coil is relatively far away the transmit coil (500mm), the coupling voltage of the coupling coil on top of the center is relatively large. In general, as the distance increases, the coupling voltage will be reduced. According to this relationship, a certain distance corresponds to a specific coupling voltage, so we can use the coupling voltage to control the distance between transmit coil and coupling coil.

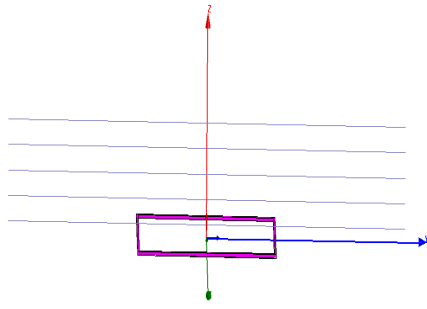


(a) Height of 10mm

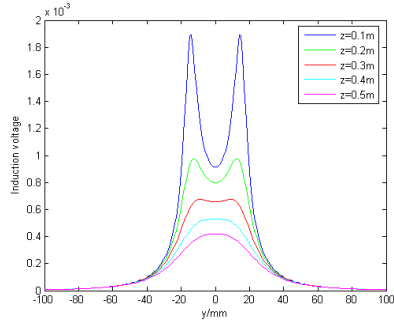


(b) Height of 500mm

Fig. 3 The distribution of induction voltage of the coupling coil in two different heights.

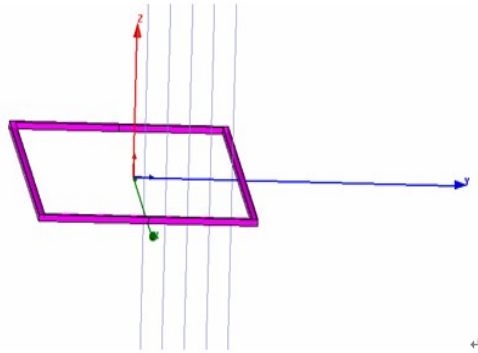


(a)

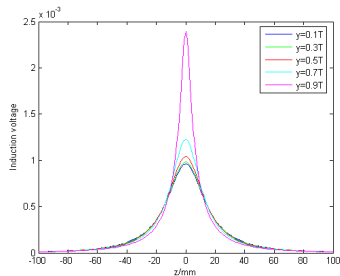


(b)

Fig. 4 The distribution curve of the induction voltage's amplitude at the line which is parallel to transmit coil



(a)



(b)

Fig. 5 The decay curve of the induction voltage's amplitude at the line which is perpendicular to transmit coil

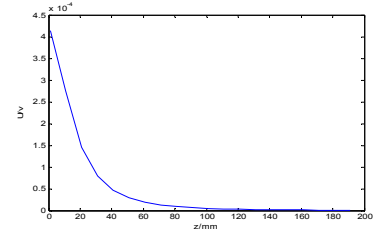


Fig. 6 The coupling voltage vs the distance

We used HFSS simulation software to describe the segment's position near the coil as shown in Fig.4 (a) and Fig.5 (a). The length of the parallel segments and vertical segments are all 200 mm. Since the length of the transmit coil is 70mm, then $T = l_2 / 2 = 70 / 2 = 35\text{mm}$. The top curve in Fig.4 (b) is the distribution curve of induction voltage of the parallel segment with the height of $z = 0.1T = 3.5\text{mm}$, which has two peak value about $1.9 \times 10^{-3}\text{V}$. The closer to the transmit coil the parallel segment is, the bigger the induction voltage is. As shown in Fig.4 (b), the induction voltage decreases with the value of z , i.e. the parallel segment is far away from the transmit coil. Fig.5 shows that the vertical segment will be far away from the origin of coordinates but close to the square coil with the increase of y value. For instance, when $y = 0.9T = 0.9 \times 70 / 2 = 31.5\text{mm}$, there is a bigger induction voltage. Moreover, in the same vertical line, the bigger the absolute value of z is, which means the further away from the transmit coil, the smaller the induction voltage is.

From the above analysis, we can conclude a typical coupling voltage in a typical distance away from the plane of transmit coil. Thus the coupling voltage can be used to control the distance between the transmit coil and coupling coil. The relationship between the coupling voltage and the distance from the transmit coil to the coupling coil is shown in Fig.6.

On the basis of magnetic coupling principle, the instantaneous induction voltage v_2 can be calculated in detail as follows.

$$\begin{aligned}
 v_2 &= -\frac{d\Psi_{21}}{dt} \\
 &= -N_2 \frac{d}{dt} [B \Delta S] \\
 &= -[N_2 \frac{N_1 \mu_0 I_1 l_2}{\pi} \left(\frac{1}{(l_1^2 + z^2) \sqrt{l_1^2 + l_2^2 + z^2}} + \frac{1}{(l_1^2 + z^2) \sqrt{l_1^2 + l_2^2 + z^2}} \right) a_1 b_1] \frac{di}{dt}
 \end{aligned} \tag{12}$$

where Ψ_{21} is the mutual inductance magnetic flux chain, i is the exciting current of transmit coil, ϕ_{21} is magnetic flow for i passing through the coupling coil, a_1 is length of coupling coil, b_1 is width of coupling coil, z is distance between transmit coil and coupling coil, N_1 is number of turns of transmit coil, N_2 is number of turns of coupling coil. In (12), the negative sign means that the mutual inductance voltage and the mutual inductance magnetic flux chain of coupling

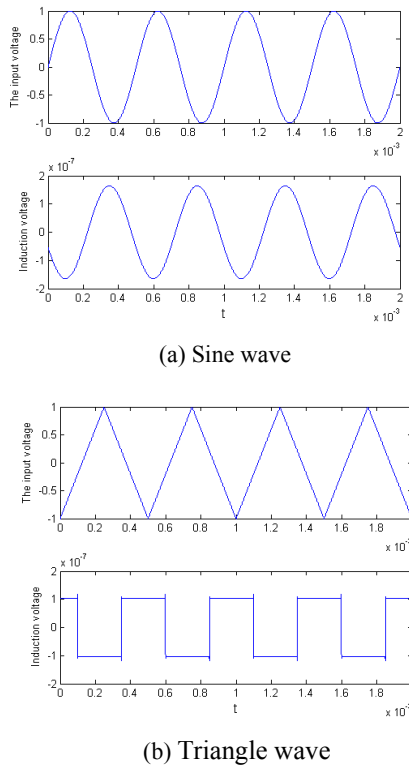


Fig. 7 The induction voltage of coupling coil in different input waveforms

coil do not satisfied right-hand screw rule. When the driving source is the voltage source, using the formula $I = U / \sqrt{R^2 + (\omega L)^2}$, we can calculate the effective value of i .

When the transmit coil is rectangle, the frequency is 2kHz, the distance of transmit coil and coupling coil is 0.5m, and the input waveform is sine wave, the coupling voltage caused by coupling coil is showed in Fig.7(a). When the transmit coil inputs triangular wave, the coupling voltage is shown in Fig.7(b).

As shown in Fig. 7(a), the coupling voltage waveform is a cosine wave when the input waveform is a sine wave. It is because the formula which calculates the induction voltage has a minus sign that make the phase change of 180 degrees. The peak value of the coupling voltage is 0.17uV, as shown in Fig.7(b), when the driving voltage is a triangular wave, coupling voltage wave form is square wave, the peak value of coupling voltage is 0.1uV. Thus the coupling voltage of the sine wave is bigger than triangular wave in the same height and same input voltage amplitude.

V. CONCLUSION

On the basis of a magnetic coupling model in the mobile payment system, and then using the electromagnetic theory and Monte Carlo simulation method, we conclude that the magnetic flux density will decrease when the height of

transmit coil increases. The induction voltage of coupling coil in different space position shows that the closer to the coupling coil the transmit coil is, the bigger the coupling voltage is. When a different voltage waveform is input into the transmit coil (sine wave or triangle wave) with the same voltage amplitude, the coupling voltage caused by sine wave is bigger than that of triangular wave. However, we suggest to use triangular wave in a practical mobile payment system. The simulation results have provided a useful guidance for our design of mobile payment system.

ACKNOWLEDGMENT

This paper was supported by the Foundation of Nantong Technologies Co, LTD, National Natural Science Foundation of China (No.60972037), the Fundamental Research Program of Shenzhen City (No.JC200903120101A and No. JC201005250067A) and the S&T Research Program of Nanshan District (No.2009045).

REFERENCES

- [1] Phone Lin, Hung-yueh Chen, Yuguang Fang et al, "A Secure Mobile Electronic Payment Architecture Platform for Wireless Mobile Networks," IEEE Trans. On Wireless Communications, 2008, vol.7, no.7, pp.2705-2713.
- [2] http://tech.ifeng.com/magazine/detail_2010_04/02/449127_0.shtml.
- [3] Varshney U, "Mobile payments," Computer, 2002, vol.35, no.12, pp.120-121.
- [4] Rivest R. L. and Shamir A., "PayWord and MicroMint: two simple micropayment schemes," IEEE Trans. On Vehicle Technology, 2003, vol.52, no.1, pp.132-141.
- [5] Zongkai. Yang, Wenming Lang, and Yunmeng Tan, "A new fair micropayment system based on hash chain," IEEE International Conference on e-Technology, e-Commerce and e-Service (EEE'04), 2004, pp.139-145.
- [6] Parul Oswal, Michelle Foong, RFID Vs Contactless Smart cards – An unending debate, Frost & Sullivan, Asia Pacific, 2006.
- [7] Y. C. Or, K. W. Leung, R. Mitra, and K.V.S. Rao, "Platform tolerant RFID tag antenna," IEEE Int. Symp.on Antennas Propagat., 2007, pp.5491-5494.
- [8] Mohammed A Qadeer, Nadeem Akhtar, Shalini Govil, "A Novel Scheme for Mobile Payment using RFID-enabled Smart SIMcard," Proc. IEEE International Conference on Future Computer and Communication, 2009, 339-343.
- [9] McDonalds, DoCoMo deal allows mobile payment for Happy Meals, <http://www.selfserviceworld.com/article.php?id=19933>.
- [10] Junwei Zou, Chu Zhang, Chongbo Dong et al, "Mobile payment based on RFID-SIM card," 2010 10th IEEE International Conference on Computer and Information Technology (CIT 2010), 2010, pp.2052-2054.
- [11] Xiaodan Wu, Yunfeng Wang, Junbo Bai et al, "RFID application challenges and risk analysis," 2010 IEEE 17th International Conference on Industrial Engineering and Engineering Management (IE&EM), 2010, pp.1086-1090.
- [12] Helin Zhang, Dawei Li, "The Application and system design for RFID technology in China urban public traffic management," 2011 International Conference on E -Business and E -Government (ICEE), , 2011, pp.1-4.
- [13] A. Wille, M. Broll , S. Winter, "Phase difference based RFID navigation for medical applications," 2011 IEEE International Conference on RFID, 2011, pp.98-105.
- [14] Youbok Lee, "Antenna Circuit Design for RFID Applications," Microchip Technology Inc., 2003.